ACTA MECHANICA SINICA (English Series), Vol.17, No.1, February 2001 ISSN 0567-7718
The Chinese Society of Theoretical and Applied Mechanics
Chinese Journal of Mechanics Press, Beijing, China
Allerton Press, INC., New York, U.S.A.

PARTICULATE SIZE EFFECTS IN THE PARTICLE-REINFORCED METAL-MATRIX COMPOSITES*

Wei Yueguang (魏悦广)
(*LNM, Institute of Mechanics, Chinese Academy of Sciences, Beijing* 100080, *China*)

ABSTRACT: The influences of particle size on the mechanical properties of the particulate metal matrix composite are obviously displayed in the experimental observations. However, the phenomenon can not be predicted directly using the conventional elastic-plastic theory. It is because that no length scale parameters are involved in the conventional theory. In the present research, using the strain gradient plasticity theory, a systematic research of the particle size effect in the particulate metal matrix composite is carried out. The roles of many composite factors, such as: the particle size, the Young's modulus of the particle, the particle aspect ratio and volume fraction, as well as the plastic strain hardening exponent of the matrix material, are studied in detail. In order to obtain a general understanding for the composite behavior, two kinds of particle shapes, ellipsoid and cylinder, are considered to check the strength dependence of the smooth or non-smooth particle surface. Finally, the prediction results will be applied to the several experiments about the ceramic particle-reinforced metal-matrix composites. The material length scale parameter is predicted.

KEY WORDS: size effect, strain gradient plasticity, the particle-reinforced metal-matrix composite

1 INTRODUCTION

Due to the potential applications of the particle-reinforced metal-matrix composites (PMMC), the respective researches have been paid much attention in the past decades. The researches include: the Young's modulus effect of the particle, the particle aspect ratio effect, the particle volume fraction effect and size effect, as well as the matrix material strain hardening effect. Some important conclusions have been obtained in the research and manufacturing regions. The results of previous researches either experimental or numerical have shown that all effects mentioned above have an important influence on the composite properties. Especially by the numerical simulations using the cell models[1,2], some detailed quantitative information about the composite strength has been built up. The composite always has either the high flow stress or the high strengthening because a higher triaxiality stress exists within the matrix region near the particle surface under loading[1]. The particulate aspect ratio and the volume fraction, as well as the strain hardening exponent of the

Received 21 April 1999, revised 19 September 1999
* The project supported by the National Natural Science Foundation of China (19891180, 19925211) and by the Chinese Academy of Sciences (KJ951-1-201) and "Bai Ren" plan

matrix material had important influences on the composite properties, and some quantitative relations were developed[1,2] by using cell models. The predicted results are consistent with experimental results. In addition, a self-consistent analytical model has been used successfully to predict the behavior of the PMMC[3]. More recently, a systematic experimental research for the metallic fiber reinforced Al-alloy matrix for a series of the volume fraction of fiber was carried out[4]. The results showed that the high material strengthening was obtained; however the composite flexibility was quite poor. On the researches of the particle size effects, the experimental results[5~10] showed that the strength of the PMMC was sensitive to the particle size. The conclusion was that the smaller the particle, the higher the composite strength. In order to predict the particle size effects, some analytical models were developed[11,12]. A motivated combination model of the effective medium approach with the dislocation plasticity mechanism was presented based on the linkage theories of micro- and macro-scales, which was used to investigate the particle size effects. In order to obtain a perfect comparison with the experimental result, the particle cracking was introduced in the analysis[11]. Another combination model of the incremental self-consistent method with the particle damage mechanism was used to study the particle size effect[12]. Previously, the difference between results of the large particle sizes and ones with the small particle sizes was thought due to the more damage included in the large particle case. Comparing with the researches about other factor effects, the research of the particle size effects has not been paid much attention because the size effect research is very difficult and no proper theories can be used. As well known, the conventional elastic-plastic theory can not be used to predict the particle size effects effectively, because no length scale parameter is included in the theory. Besides the size-effect phenomena in the PMMC, these phenomena have been found in many research regions, such as: in the micro-indentation test[13~15], in the micro-torsion test of column[16], as well as the interface separation of metal/ceramic system[17]. The size effect phenomena for metal jointing with ceramic composite materials were thought as coming up within a linkage region between the microscopic region and the macro-scale region, where the conventional theory can not be used. In order to describe the size effects, in recent years, several strain gradient plasticity theories have been presented and developed[18~20] based in the frame of deformation theory. At the same time, an incremental theory of strain gradient plasticity has been developed and successfully used to the growing crack analysis[21]. In the strain gradient plasticity theory, a very marked characteristic is that a length scale parameter is introduced, by which the size effect phenomena can be described.

In the present research, the Fleck-Hutchinson's strain gradient plasticity theory[18] is used to simulate the mechanical response of the PMMC. A detailed analysis of the particle size effects is carried out. Adopting the strain gradient plasticity theory, the composite stress-strain curves will depend on the following parameters: the Young's modulus ratio of both particle and matrix; Poisson's ratio; particle volume fraction; particle aspect ratio; strain hardening exponent of matrix material; a normalized particle volume with the material length scale parameter. Therefore, the purpose of the present research is to set up a series stress-strain relations depending on all the parameters mentioned above, especially on the normalized particle volume with material length scale parameter. In the present analysis, a cell model is adopted, and two kinds of particle shapes: ellipsoid and cylinder are considered. Finally, using analysis results to the experiments, the material length scale parameter is predicted.

2 STRAIN GRADIENT PLASTICITY

The general form of the deformational theory of strain gradient plasticity with compressibility has not been found in literature. Here a brief description is provided in the following subsections.

2.1 Constitutive Relations

The definitions of the strain and strain gradient are given by

$$\varepsilon_{ij} = \frac{1}{2}(u_{i,j} + u_{j,i}) = \varepsilon_{ij}^e + \varepsilon_{ij}^p \qquad \eta_{ijk} = u_{k,ij} = \eta_{ijk}^e + \eta_{ijk}^p \tag{1}$$

The expressions related with the constitutive relation are listed as follows

$$\begin{aligned}
&W^e = E\Big(\frac{\nu}{2(1+\nu)(1-2\nu)}\varepsilon_{kk}^{e2} + \frac{1}{2(1+\nu)}\varepsilon_{ij}^e\varepsilon_{ij}^e + \sum_{I=1}^{4} L_I^{e2}\eta_{ijk}^{e(I)}\eta_{ijk}^{e(I)}\Big)\\
&\sigma_{ij} = \partial W^e/\partial\varepsilon_{ij}^e, \qquad \tau_{ijk} = \partial W^e/\partial\eta_{ijk}^e\\
&\Xi = \sqrt{\frac{2}{3}\varepsilon'_{ij}\varepsilon'_{ij} + \sum_{I=1}^{3} L_I^2\eta_{ijk}^{(I)}\eta_{ijk}^{(I)}}\\
&\Sigma = \sqrt{3J_2} = \sqrt{\frac{3}{2}\sigma'_{ij}\sigma'_{ij} + \sum_{I=1}^{3} L_I^{-2}\tau_{ijk}^{(I)}\tau_{ijk}^{(I)}}\\
&\eta_{ijk}^{(I)} = T_{ijklmn}^{(I)}\eta_{lmn}, \qquad \tau_{ijk}^{(I)} = T_{ijklmn}^{(I)}\tau_{lmn}\\
&\varepsilon_{ij}^p = \frac{3}{2h^p}\frac{\partial J_2}{\partial\sigma_{ij}} = \frac{3}{2h^p}\sigma'_{ij}\\
&\eta_{ijk}^p = \frac{3}{2h^p}\frac{\partial J_2}{\partial\tau_{ijk}} = \frac{1}{h^p}\sum_{I=1}^{3} L_I^{-2}T_{ijklmn}^{(I)}\tau_{lmn}\\
&h^p = \Sigma/(\Xi - \Sigma/E)
\end{aligned} \tag{2}$$

where Σ and Ξ are the equivalent stress and strain, respectively; L_I^e and $L_I(I = 1, 4)$ are the material micro-length scales for elastic case and plastic case, respectively. From the discussion in [18], there exists a general relation among the material length scale parameters

$$L_1 = L \qquad L_2 = \frac{1}{2}L \qquad L_3 = \sqrt{\frac{5}{24}}L \tag{3}$$

In addition, take $L_4 = L/2$. Similarly, Eq.(3) is valid also for the elastic strain gradient case, with L being replaced with L^e. Moreover, the previous research has shown that the solution is insensitive to the value of L^e/L within the range $0 < L^e/L < 1$[21]. Therefore, in the present analysis, we take $L^e/L = 0.5$. In formula (2), h^p is the equivalent plastic modulus. Consider that the matrix is made of a plastic material with a strain-hardening exponential law

$$\begin{aligned}
&\Xi = \Xi_0(\Sigma/\sigma_Y) &\quad \Sigma \le \sigma_Y\\
&\Xi = \Xi_0(\Sigma/\sigma_Y)^{1/N} &\quad \Sigma > \sigma_Y
\end{aligned} \tag{4}$$

we have

$$h^p = E\{(\Sigma/\sigma_Y)^{1/N-1} - 1\}^{-1} \tag{5}$$

$T^{(I)}_{ijklmn}(I = 1,4)$ in formulas (2) is the projection tensor in strain gradient plasticity, and its detailed expressions have been given in [21]. Thus, by using formulas (1) and (2) and the projection tensor normality, the compressible general form of the deformational theory of strain gradient plasticity can be derived as

$$\begin{aligned} \sigma_{ij} &= \frac{E}{1+\nu+\frac{3}{2}E/h^p}\varepsilon_{ij} + \frac{1}{3}\Big(\frac{E}{1-2\nu} - \frac{E}{1+\nu+\frac{3}{2}E/h^p}\Big)\varepsilon_{kk}\delta_{ij} \\ \tau_{ijk} &= 2E\Big\{\sum_{I=1}^{3}\frac{L_I^2}{L_I^2/L_I^{e2} + 2E/h^p}T^{(I)}_{ijklmn} + L_4^{e2}T^{(4)}_{ijklmn}\Big\}\eta_{lmn} \end{aligned} \tag{6}$$

2.2 The Equilibrium or Variational Relation

Frequently, the equilibrium equation can be described by the displacement-based variational relation. The finite element method (or numerical method) is readily developed. The displacement variational relation for the strain gradient plasticity theory is given by[18]

$$\int_V (\sigma_{ij}\delta\varepsilon_{ij} + \tau_{ijk}\delta\eta_{ijk})\mathrm{d}V = \int_V f_k\delta u_k \mathrm{d}V + \int_S t_k\delta u_k \mathrm{d}S + \int_S r_k(D\delta u_k)\mathrm{d}S \tag{7}$$

Based on Eq.(7), the traction on surface S is defined by

$$t_k = n_i\Big(\sigma_{ik} - \frac{\partial\tau_{ijk}}{\partial x_j}\Big) + n_i n_j \tau_{ijk}(D_p n_p) - D_j(n_i\tau_{ijk}) \tag{8}$$

and the surface torque is defined by $r_k = n_i n_j \tau_{ijk}$; The gradient operators are defined by

$$D_j = \frac{\partial}{\partial x_j} - n_j n_k\frac{\partial}{\partial x_k} \qquad D = n_k\frac{\partial}{\partial x_k} \tag{9}$$

where n_i is the directional cosine on the surface S.

3 MATERIAL MODEL AND FINITE ELEMENT METHOD

3.1 Material Model

Consider two kinds of particles, ellipsoid and cylinder. The simplified cell models are shown in Fig.1. For the axial-symmetrical condition, only the one-fourth of material region needs to be considered as shown in Fig.1(c). The normalized cell sizes (the material length parameter L, see Eq.(3), is taken as the normalized length quantity) for ellipsoidal particle read

$$A = \Big(\frac{3k}{4\pi}\Big)^{1/3}\frac{V_P^{1/3}}{L} \qquad B = \frac{A}{k} \qquad R = \Big(\frac{k}{2\pi f_P}\Big)^{1/3}\frac{V_P^{1/3}}{L} \qquad H = \frac{R}{k} \tag{10}$$

where V_P and f_P are the particle volume and volume fraction, respectively

$$k = A/B = R/H \tag{11}$$

is the particle and cell aspect ratio. Note that the cell volume can not take unity as usual, because the reference length is L, instead of the usual cell size. Therefore, three independent

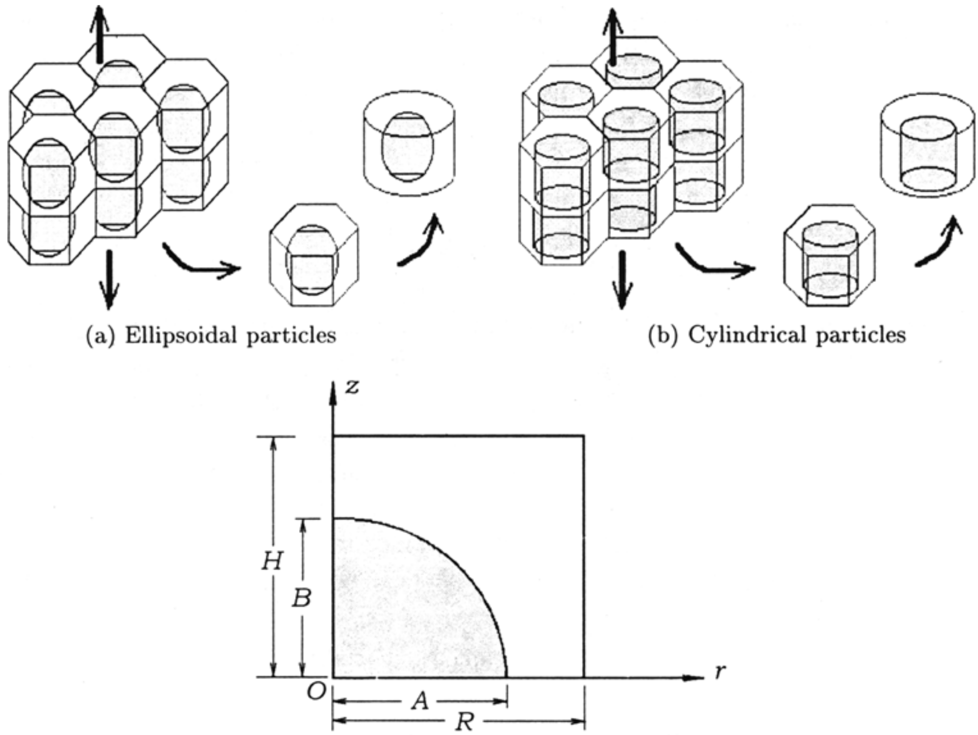

(a) Ellipsoidal particles (b) Cylindrical particles

(c) Cell geometry

Fig.1 The cell models

parameters for the cell geometry description are needed from Eq.(10), instead of only two independent parameters for the usual cell model description. From dimensional analysis, additional composite parameter, $V_P^{1/3}/L$, describing the cell size and the strain gradient effects, must appear in the analysis inevitably.

Similarly, for the cylindrical particle case, we have

$$A = \left(\frac{k}{\pi}\right)^{1/3} \frac{V_P^{1/3}}{L} \qquad B = \frac{A}{k} \qquad R = \left(\frac{k}{\pi f_P}\right)^{1/3} \frac{V_P^{1/3}}{L} \qquad H = \frac{R}{k} \tag{12}$$

The boundary conditions (see Fig.1 (c)) are described as

$$\begin{array}{llll} u_z = 0 & T_r = 0 & & \text{on} \quad z = 0 \\ u_z = \varepsilon_c H & T_r = 0 & & \text{on} \quad z = H \\ u_r = \text{const} & T_z = 0 & \displaystyle\int_0^H T_r \mathrm{d}z = 0 & \text{on} \quad r = R \end{array} \tag{13}$$

In the present analyses, the metal matrix is treated as an elastic-plastic material considering strain gradient plasticity, see formulas (4) to (6). The particle is treated as an elastic material with Young's modulus E_P and Poisson's ratio ν_P.

The parameter dependence of the stress-strain relations of the PMMC can be written as

$$\frac{\sigma_c}{\sigma_Y} = F\left(\varepsilon_c, \ \frac{E_P}{E}, \ f_P, \ k, \ N, \ \frac{V_P^{1/3}}{L}, \ \frac{E}{\sigma_Y}, \ \nu, \ \nu_P\right) \tag{14}$$

There are many parameters included in Eq.(14). For the simplification, in the present analyses we consider $(E/\sigma_Y, \nu, \nu_P) = (300, 0.3, 0.3)$. Note that the parameter, $V_P^{1/3}/L$, takes a dual-meaning: the particle size (when L is fixed) and the strain gradient strength (when $V_P^{1/3}$ is fixed). Therefore, when the composite parameter value $V_P^{1/3}/L$ is big, both cases of the large particle size and the small strain gradient effect will be described; especially, when the parameter value tends to the infinity, the problem is degraded to the conventional cell model case (no strain gradient effect). Inversely, when its value is small, the case corresponds to the small particle or large strain gradient effect.

3.2 Finite Element Method of the Strain Gradient Plasticity

Generally speaking, when the strain gradient effect is considered, the conventional finite element method fails and a special finite element method, where the pure displacement derivatives are taken as nodal variables, is needed[21~23]. However, when strain gradients are stretching-dominated, the valid result can be obtained by using the nine-node iso-parametric displacement element (see [21], [23]). Obviously, for the PMMC case under the boundary conditions as Eq.(13), the strain gradient deformation is truly stretching-dominated. Therefore, in the present analyses, we adopt the nine-node iso-parametric displacement element and a 2×2 Gauss integral scheme.

The finite element method for using the deformational plastic theory can be described as follows:

(1) obtain the elastic solution:

(2) calculate for the higher strain-hardening exponent case through iteration, based on the elastic solution;

(3) calculate for the lower strain-hardening exponent case by iterating, based on the solution in step (2).

For example, the steps of calculating for case $N = 0.1$ can be described as follows. Firstly, obtain the elastic solution. Then, based on the elastic solution, calculate for the case $N = 0.3$ through iterating. Thirdly, taking the solution of $N = 0.3$ as an initial solution, calculate for the case $N = 0.1$ by iterating.

The element form adopted is shown in Fig.2. In the present analyses, the number of nine-node elements adopted is 1280. In Fig.2, for comparison, the cell models for two kinds of particles and for different particle volume fractions are shown.

4 RESULTS

4.1 Ellipsoidal Particle Case

Figure 3 shows the stress-strain curves of the composites for different particle volume fractions and different particle sizes when Young's modulus values of both particle and matrix are equal and the particle aspect ratio (the ratio of width with height of particle) is 0.3. From Fig.3, both the particle volume fraction and the particle size have strong effects on the composite strength. For a comparison, the case when Young's modulus ratio is equal to 3 is considered and the results are shown in Fig.4. By comparing the results of Figs.3 and 4, it is obvious that the stress-strain curves of composites are very sensitive to the

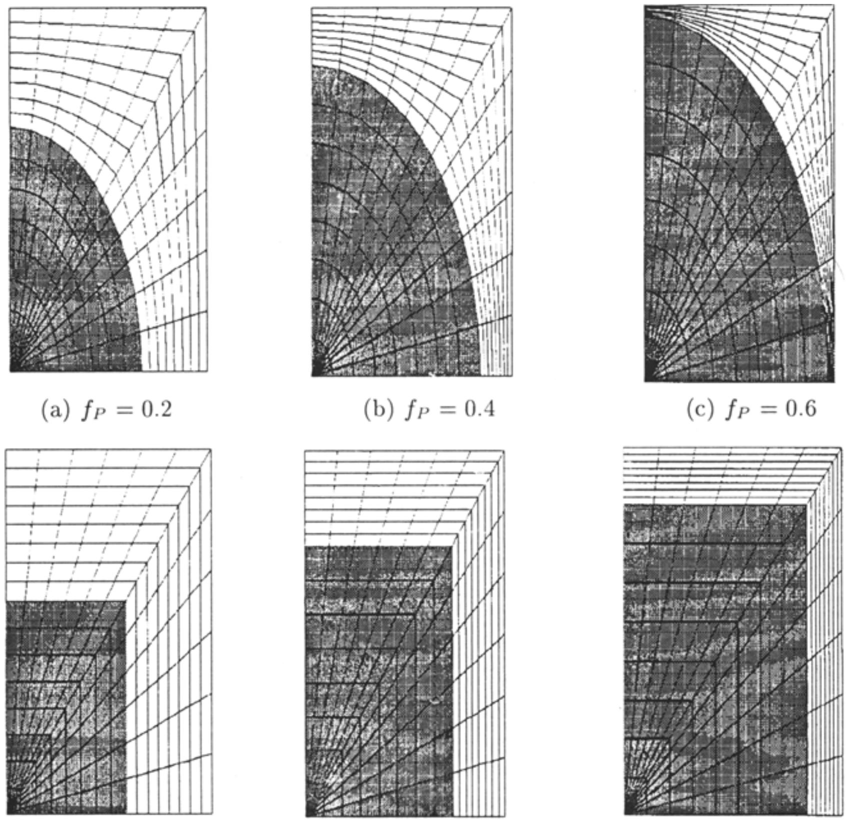

(a) $f_P = 0.2$ (b) $f_P = 0.4$ (c) $f_P = 0.6$

(d) $f_P = 0.2$ (e) $f_P = 0.4$ (f) $f_P = 0.6$

Fig.2 Two kinds of cell models for different volume fractions. (a), (b) and (c) are ellipsoidal particle; (d),(e) and (f) are cylindrical particle

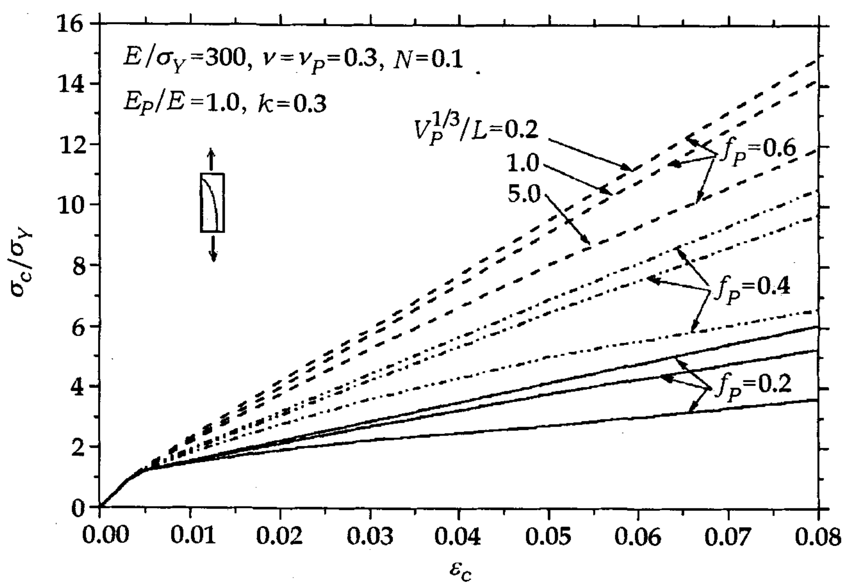

Fig.3 The dependence of the stress-strain curves of composite on the particle sizes and volume fractions when Young's modulus ratio of both particle and matrix is unity

Young's modulus ratio. The dependence of the stress-strain relations on the Young's modulus ratios for spherical particle is shown in Fig.5. From Fig.5, the stress-strain curves are also very sensitive to the particle sizes, with Young's modulus ratio increasing. Figure 6 shows that the stress-strain curves are dependent on the particle sizes and particle aspect ratios. The results in Fig.6 include the three cases with different aspect ratio: the high and thin particle shape, the spherical particle and the flat particle shape. From Fig.6, the composite strengthening is the smallest for the spherical particle case. When the particle volume fraction is fixed, for the big particle size case the composite strengths are sensitive to particle

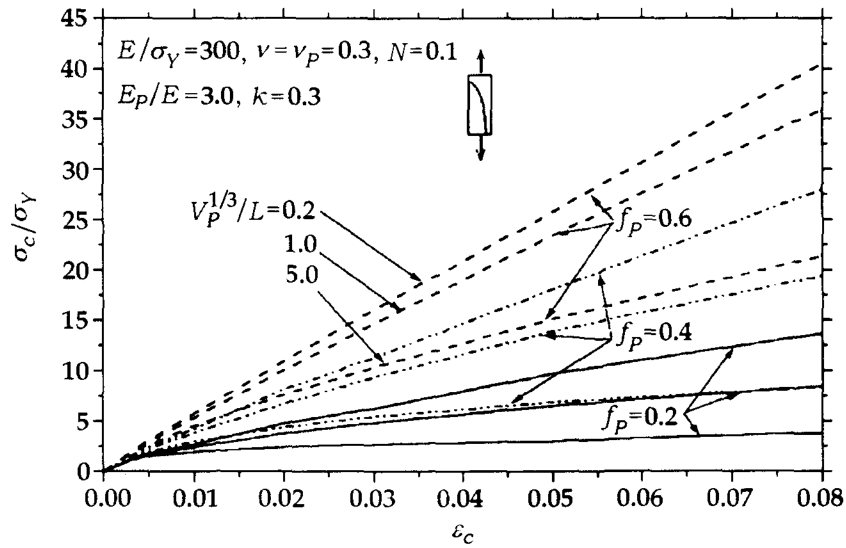

Fig.4 The dependence of the stress-strain curves of composite on the particle sizes and volume fractions when Young's modulus ratio of both particle and matrix is three

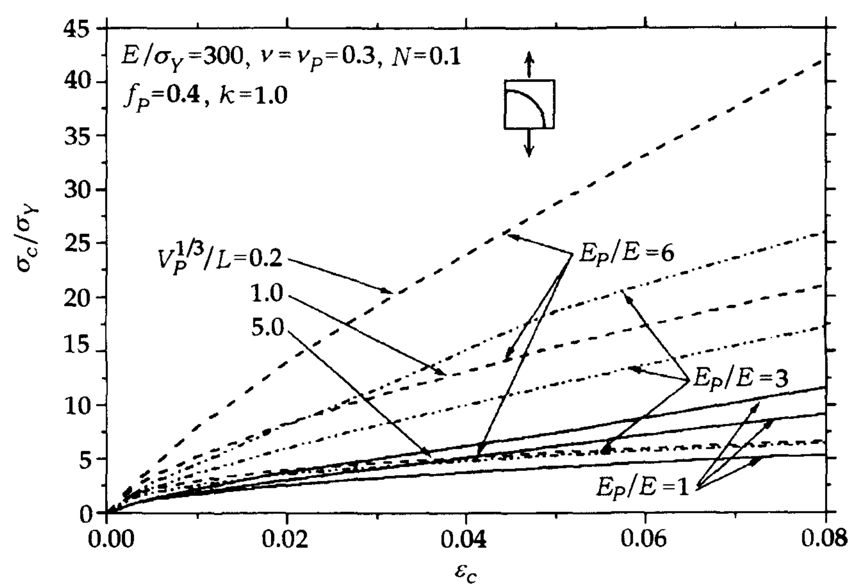

Fig.5 The dependence of the stress-strain curves of composite on the particle sizes and the Young's modulus ratios for spherical particle case

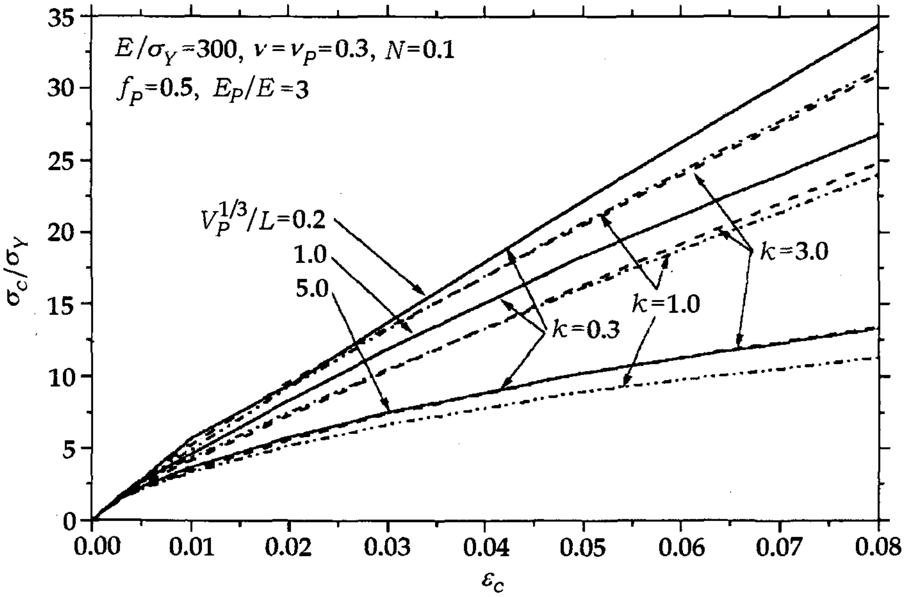

Fig.6 The dependence of the stress-strain curves of composite on the particle sizes and aspect ratio

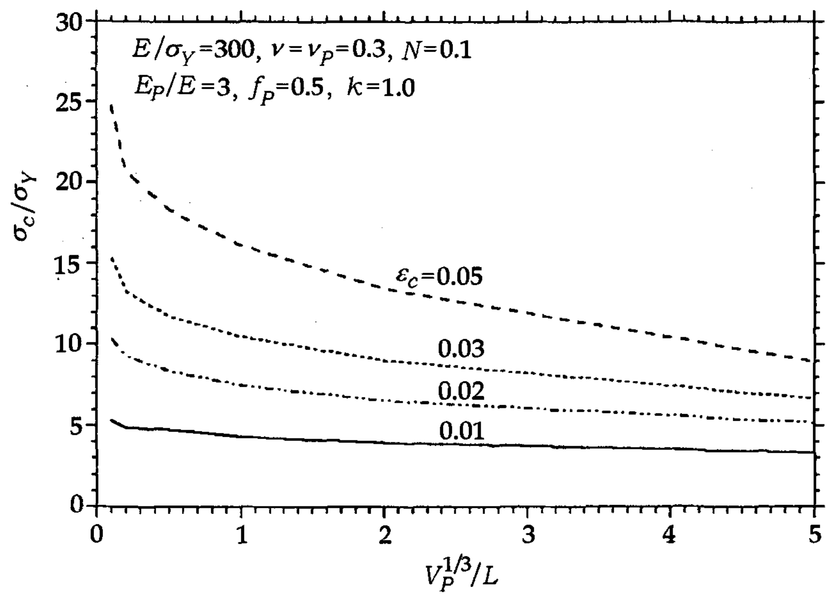

Fig.7 Variations of stress with the particle size for several strain values

aspect ratios, while with the particle size decreasing the stress-strain curves are getting to be insensitive to the particle aspect ratio. Figure 7 shows the stress variations with particle size in composite for the different strain values and the high volume fraction of the spherical particles. From Fig.7, the stress strongly depends on the particle size, especially for small particle and large composite strain. Composite strength also depends on the strain-hardening exponent of the matrix material from Fig.8 for the spherical particle case and the high particle volume fraction, when Young's modulus ratio is equal to 3.

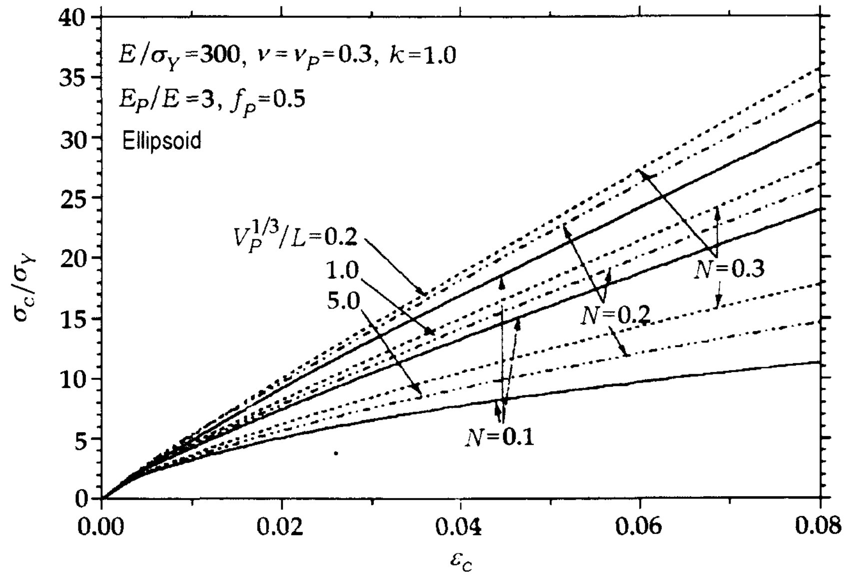

Fig.8 The dependence of the stress-strain curves of composite on the particle sizes and the strain-hardening exponents of matrix

4.2 Cylindrical Particle Case and The Result Comparison for Two Kinds of Particles

The results of the cylindrical particle case are very similar to those for ellipsoidal particle. For the cylindrical particles, the composite strength also strongly depends on the Young's modulus ratio of the particle and matrix materials, particle size and aspect ratio, particle volume fraction, as well as the strain-hardening exponent of matrix material.

It is interesting to compare the results of ellipsoidal particle with those of cylindrical particle when all other parameters are fixed. Figure 9 shows the detailed comparison of two

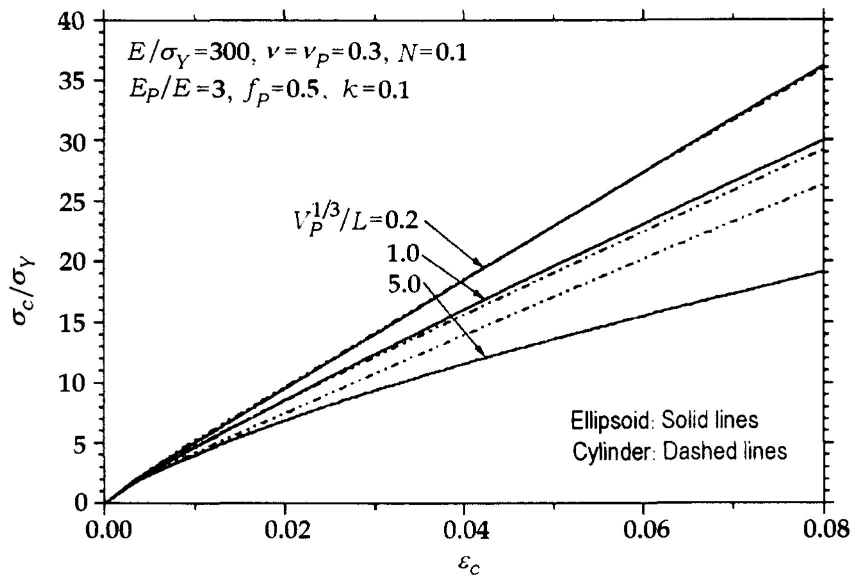

(a)

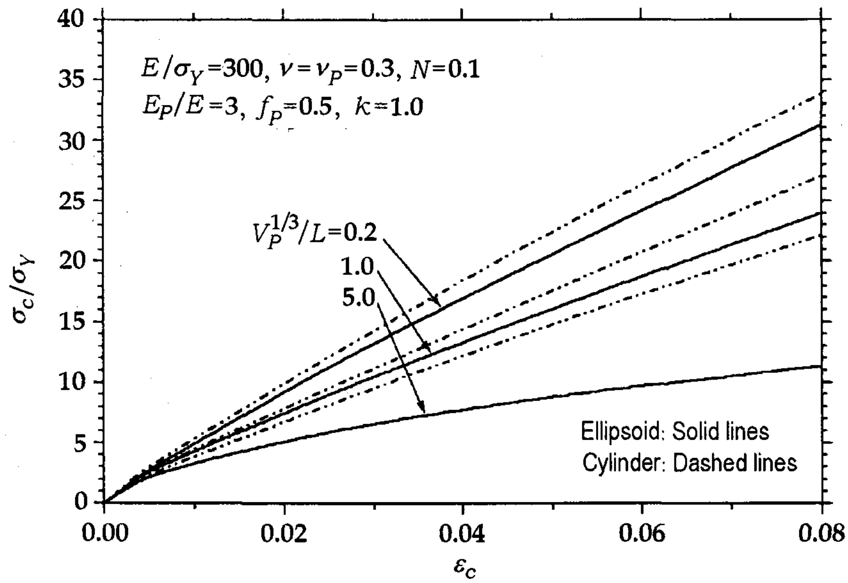

(b)

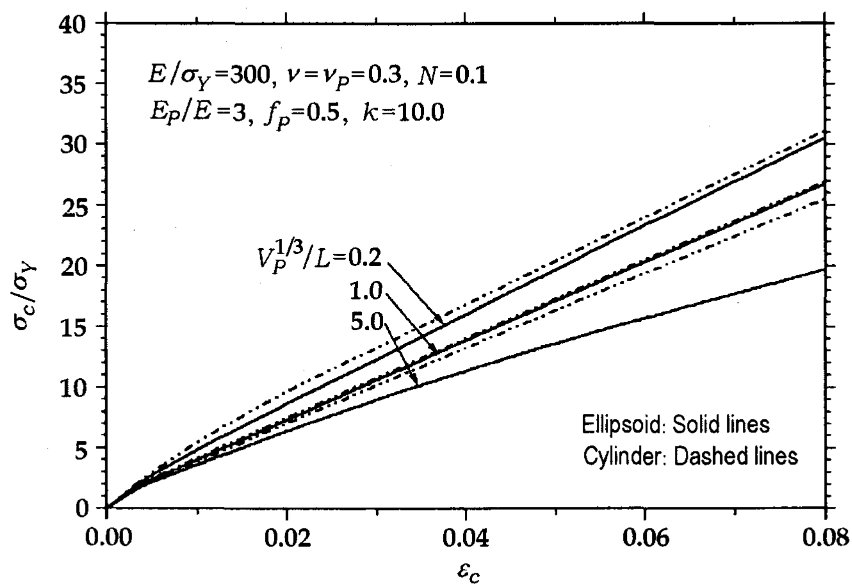

(c)

Fig.9 Detailed comparison of the results of both ellipsoidal particle case and cylindrical particle case for a series aspect ratios. From (a) to (c), k = 0.1, 1.0 and 10.0

kinds of particles for different particle aspect ratios. Comparing the three aspect ratio cases in Fig.9, the following conclusions are readily obtained: (1) When particle size is large, there is a big difference between the results of two different kinds of particles. As the particle size decreases, two results tend to become consistent with each other; (2) when particle aspect ratio is very low (k = 0.1) or very high (k = 10), the difference between two results disappears very quickly.

5 APPLICATION TO THE EXPERIMENTS OF Al-ALLOY / SiCp COMPOSITES

The analytical results obtained in the last section will be applied to the experiments of the Al-Alloy / SiCp composites. The first application is to the experiment of the Al-4wt% Mg alloy reinforced by the SiC particle[5]. The dependence of compressive stress-strain relations on the particle sizes for the higher particle volume fraction case in experiment and analysis is shown in Fig.10. The experimental result corresponds to the two particle sizes, i.e., when particle radii are 13 micron and 165 micron. The analytical results correspond to the particle radii of 16 and 160 micron. According to these particle sizes, we can determine the particle volume V_P in the analytical results. Moreover, from Fig.10, when the composite length scale L is taken as 6.45 micron, both results are consistent qualitatively and quantitatively, when the strain value is smaller than 2%. But when the strain value is larger than 2%, for small particle, the analytical results go up quickly and deviate from the experimental result. This is because that in the analytical model a perfect adhesion between particle surface and matrix is assumed and no particle fracture and damage are considered. Actually, the specimen contains always some damages and particle cracking[11,12].

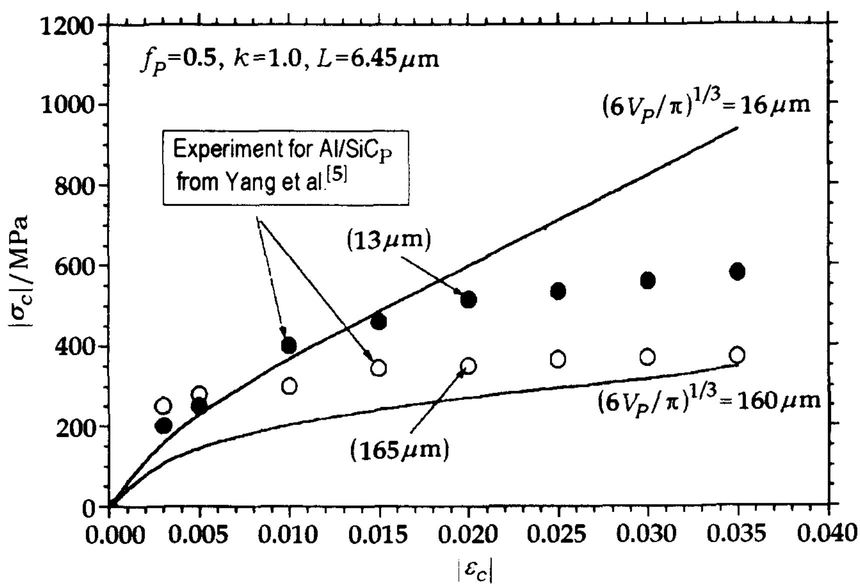

Fig.10 An application of analysis result to the experiment for Al/SiCp when particle volume fraction is high ($f_P = 0.5$)

The second application is to the experiment of the 2124Al reinforced by SiC particles[9,10]. The dependence of the compressive stress-strain curves on the particle sizes for the lower particle volume fraction from experimental result and analytical result is shown in Fig.11. From Fig.11, when the composite length scale parameter L is taken as 4.25 micron, both results are consistent qualitatively and quantitatively.

Roughly, from above applications the material length scale parameter L is dependent on the particle volume fraction. For the pure aluminum, the material length scale parameter is about 1.5 micron from micro-indentation test and analyses[24].

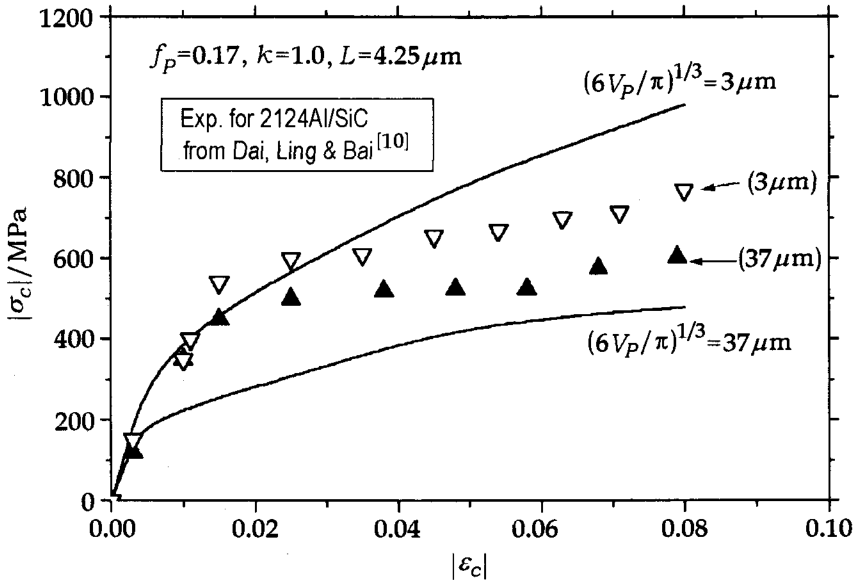

Fig.11 Another application of analysis result to the experiment for 2124Al/SiC$_P$ when particle volume fraction is low ($f_P = 0.17$)

6 CONCLUDING REMARKS

The results of the present study provide some detailed quantitative information on the particulate size effects in the particle-reinforced metal-matrix composites. The results show the dependence of the composite strength on the particle size, Young's modulus of the particle, particle aspect ratio and particle volume fraction, as well as the strain-hardening exponent of matrix material. For the large particle case or for the conventional theoretical result, the composite strength is strongly dependent on the particle aspect ratio. With the particle size decreasing, the composite strength increases and weakly depends on the particle aspect ratio. Another important conclusion is that for the large particle or for the conventional theoretical result, the composite strength is strongly dependent on the particle shapes, ellipsoid or cylinder, while with particle size decreasing, the results for both cases (ellipsoid and cylinder) tend to be independent on the particle shapes. Especially for the very big particle aspect ratio or for the very small particle aspect ratio, the difference between two results is very small. Through applications of analyses to the experiments for Al-alloy reinforced by SiC particles for the higher particle volume fraction and lower particle volume fraction, a systematic value of the material length scale parameter is predicted. On the other hand, the present analyses and the applications suggest that for large strain case, in order to simulate the experiments using strain gradient plasticity perfectly, the damage or particle cracking must be considered.

From the last section, there is a conclusion that the material length scale parameter L is dependent on the particle volume fraction. This conclusion is readily understood, because the composites reinforced with different volume fraction particles will have different macroscopic properties. From continuum mechanics point of view, the composites of metal/ceramic consisting of the different volume fraction ceramic particles could be thought as the different macroscopic materials, so that they should have different material length scale parameter values. Certainly, this is still open to question and the further validation is needed.

REFERENCES

1 Christman T, Needleman A, Suresh S. An experimental and numerical study of deformation in metal ceramic composites. *Acta Metall Mater*, 1989, 37: 3029~3050

2 Bao G, Hutchinson J W, McMeeking R M. Particle reinforcement of ductile matrices against plastic flow and creep. *Acta Metall Mater*, 1991, 39: 1871~1882

3 Corbin S F, Wilkinson D S. The influence of particle distribution on the mechanical response of a particulate metal-matrix composite. *Acta Metall Mater*, 1994, 42: 1311~1318

4 Boland F, Colin C, Salmon C, et al. Tensile flow properties of Al-based matrix composites reinforced with a random planar network of continuous metallic fibres. *Acta Mater*, 1998, 46: 6311~6323

5 Yang J, Cady C, Hu M S, et al. Effects of damage on the flow strength and ductility of a ductile Al-alloy reinforced with SiC particuletes. *Acta Metall Mater*, 1990, 38: 2613~2619

6 Kamat S V, Rollett A D, Hirth J P. Plastic-deformation in Al-alloy matrix-alumina particulate composites. *Scripta Metall Mater*, 1991, 25: 27~32

7 Lloyd D J. Particle-reinforced aluminum and magnesium matrix composite. *Int Mater Rev*, 1994, 39: 1~23

8 Kiser M T, Zok F W, Wilkinson D S. Plastic flow and fracture of a particulate metal matrix composites. *Acta Mater*, 1996, 44: 3465~3476

9 Ling Z. Deformation behavior and microstructure effect in 2124Al/SiC$_P$ composite. *J Comp Mater*, 2000, 34: 101~115

10 Dai L H, Ling Z, Bai Y L. A strain gradient-strengthening law for particle reinforced metal matrix composites. *Scripta Mater*, 1999, 41: 245~251

11 Nan C W, Clarke D R. The influence of particle size and particle fracture on the elastic/plastic deformation of metal matrix composites. *Acta Mater*, 1996, 44: 3801~3811

12 Maire E, Wilkinson D S, Embury D, et al. Role of damage on the flow and fracture of particulate reinforced alloys and metal matrix composites. *Acta Mater*, 1997, 45: 5261~5274

13 Stelmashenko N A, Walls M G, Brown L M, et al. Microindentations on W and Mo oriented single-crystals-an STM study. *Acta Metall Mater*, 1993, 41: 2855~2865

14 Ma Q, Clarke D R. Size-dependent hardness of silver single-crystals. *J Mater Res*, 1995, 10: 853~863

15 McElhaney K W, Vlassak J J, Nix W D. Determination of indenter tip geometry and indentation contact area for depth-sensing indentation experiments. *J Mater Res*. 1998, 13: 1300~1306

16 Fleck N A, Muller G M, Ashby M F, et al. Strain gradient plasticity-theory and experiment. *Acta Metall Mater*, 1994, 42: 475~487

17 Evans A G, Hutchinson J W, Wei Y. Interface adhesion: effects of plasticity and segregation. *Acta Mater*, 1999, 47: 4093~4113

18 Fleck N A, Hutchinson J W. Strain gradient plasticity. *Adv in App Mech*, 1997, 33: 295~361

19 Aifantis E C. On the microstructural origin of certain inelastic models. *J Eng Mater Tech*, 1984, 106: 326~330

20 Gao H, Huang Y, Nix W D, et al. Mechanism-based strain gradient plasticity - I. Theory. *J Mech Phys Solids*, 1999, 47: 1239~1263

21 Wei Y, Hutchinson J W. Steady-state crack growth and work of fracture for solids characterized by strain gradient plasticity. *J Mech Phys Solids*, 1997, 45: 1253~1273

22 Xia Z C, Hutchinson J W. Crack tip fields in strain gradient plasticity. *J Mech Phys Solids*, 1996, 44: 1621~1648

23 Chen J Y, Wei Y, Huang Y, et al. The crack tip fields in strain gradient plasticity: the asymptotic and numerical analyses. *Eng Fract Mech*, 1999, 64: 625~648

24 Wei Y, Wang X, Wu X, et al. Theoretical and experimental researches of size effect in micro-indentation test. *Science in China* (Series A), 2001, 44: 74~82